-Technical paper-

SEISMIC PERFORMANCE OF FRAME UNDER LARGE CYCLIC DEFORMATION AND AXIAL LOAD VARIATION

Hakim BECHTOULA[*1], Masanobu SAKASHITA[*1], Susumu KONO[*2], Fumio WATANABE[*3]

ABSTRACT: Two 1/4-scale RC model frames with two stories and one span were subjected to cyclic, lateral loads to investigate the seismic behavior of the lower part of an eleven-story RC frame building. Variation in axial load was the variable for the two frames. The specimens maintained their lateral load carrying capacity, even at drift ratios of more than 6%. The tests provided measurements of beam elongation, column shortening and variation of shear force in each column. Good agreement was found between the analytical and experimental load-displacement relationships. Also, the analytical curvature for the frame components with respect to the frame drift matched the experimental ones well.
KEYWORDS: RC Frame, Cyclic loading, Axial load variation, Plastic hinge, Beam elongation, Damage.

1. INTRODUCTION

In the past, many researchers [1][2] have investigated the seismic behavior of columns under various types of loadings. However, fewer experiments have been performed on frame systems compared to members test, columns and beams. The presence of beams and slabs in a structure may change columns' seismic behavior dramatically. After completing the first part of a test program, in which sixteen isolated small and large-scale reinforced concrete columns were tested under various loading histories [3][4], two reinforced concrete frames with two stories and one span were tested at Kyoto University to investigate the seismic behavior of the lower part of a frame. The models represented the lower part of an eleven-story reinforced concrete frame building. These frames were designed according to the latest Japanese guidelines [5] and scaled to 1/4 to fit the loading system.

The first goal of the test program was to quantify the bending moments, axial loads and shear distributions in the first-story columns at different loading stage. The second goal was to measure the beam elongations with respect to the frame drift, and the last goal was to compare the load-displacement relationships at each story with the results of analysis.

2. EXPERIMENTAL PROGRAM

2.1 TEST SETUP

As shown in **Figure 1**, the center-to-center span of the columns was 1800 mm, and the heights of the first and second stories were 765 and 840 mm, respectively. The column cross-sections measured 270x270 mm, and the beam cross-sections measured 180x270 mm. The horizontal load was applied through a 1000 kN jack at a height of 2025 mm, which represented the distance from the base to the mid height of the third story. A 40-mm diameter PC bar passing through the column center was used to simulate the axial force of the upper stories. The PC bars applied either compression or tension to the columns by means of two jacks (one of these was a center-hole jack) set at the top of each column. The axial load target for specimen SN30 varied between $0.3 f_c' A_g$ in compression and $0.1 f_c' A_g$ in tension. For specimen SN50, the corresponding target axial loads were $0.5 f_c' A_g$ in compression and $0.2 f_c' A_g$ in tension. The axial load, N, varied linearly with respect to the applied horizontal load, H, as follows:

[*1] Department of Architecture and Architectural Systems, Kyoto University, PhD candidate, Member of JCI
[*2] Department of Architecture and Architectural Systems, Kyoto University, Associate Professor, Member of JCI
[*3] Department of Architecture and Architectural Systems, Kyoto University Professor, Member of JCI

$N = 239 \pm \Psi H\ (kN)$, where $\Psi = 2.30$ for SN30 and $\Psi = 4.59$ for SN50. Concrete and steel characteristics, as well as variation in axial load are shown in **Table 1**. To evaluate the axial load, shear load and the bending moment in each first-story column, two identical load cells were designed and calibrated before the tests. These load cells were inserted beneath the foundation, as shown on the right side of **Figure 1**.

2.2 EXPERIMENTAL RESULTS

The experimental load-displacement relationships for the two frames did not differ significantly. This can be seen clearly from **Figure 2**, which superimposes the load- displacement curves for the entire frames. Definitions of the drift ratios are provided in **Figure 4**. The maximum drift ratios for specimen SN30 were 6.08% for the whole frame, and 5.18 and 6.92% for the 1^{st} and 2^{nd} stories respectively. Similarly, the maximum drift ratios for specimen SN50 were 7.09% for the whole frame, and 5.72 and 8.33% for the 1^{st} and 2^{nd} stories respectively.

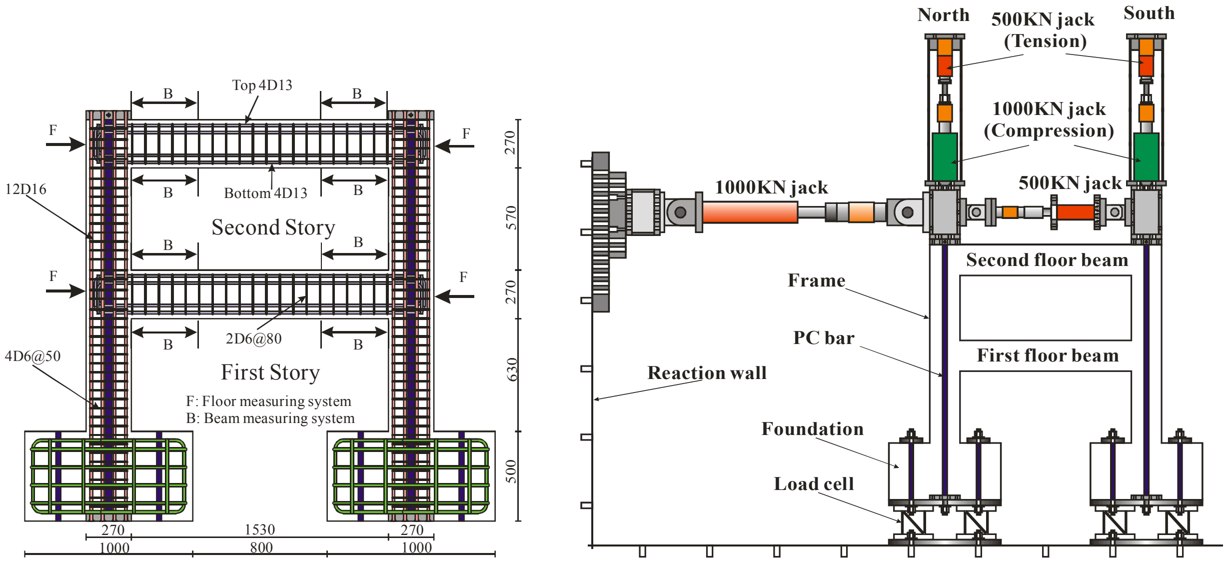

Figure 1: Reinforcement details and frame test setup

Using the load cells beneath the foundations and the PC bar forces, it was possible to determine the shear forces, axial loads and bending moments at the column bases. From **Figure 3** it can be seen that the total shear force was not carried evenly among the columns, but rather, the shear force distribution varied with the intensity of the applied axial load. The column shortening was evaluated for a height equal to the column depth, $D_c = 270\ mm$, using displacement gauges attached on each column. Columns in the 1^{st} story of frame SN30 tended to elongate rather than shorten, especially on the south side as shown in **Figure 5**. Although not shown here, the second-story columns showed nearly the same amount of shortening and elongation. In contrast, all columns in frame SN50 (both in the first and second stories) elongated more than shortened.

Table 1: Material characteristics

Frame designation	Material			Test variable -Axial load-	
	Concrete strength	Longitudinal steel	Shear rebar	Compression N/f'cD^2	Tension N/f'cD^2
SN30	31 MPa	Column 12D16 (3.27%) Fy=346 MPa Beam 8D13 (2.08%) Fy = 332 MPa	Column 4D6@50 (0.94%) Beam 2D6@80 (0.44%) Fy = 394 MPa	0.3	0.1
SN50				0.5	0.2

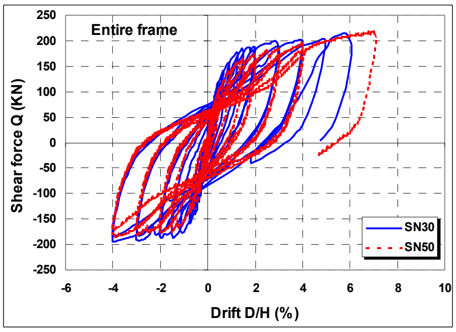

Figure 2: Load displacement relationship

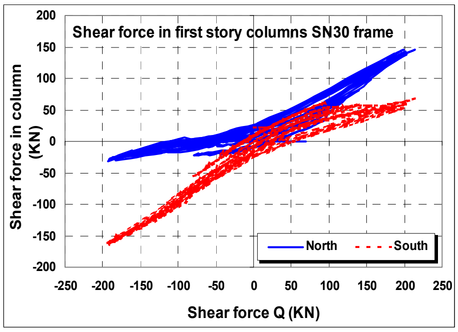

Figure 3: Shear force at the columns base -SN30 Frame-

During the test, the first and second-floor beams were severely damaged, especially near the beam-column joint. Using the displacement gauges attached directly to the beams identified by the letter "B" in **Figure 1**, the beam's length changes were evaluated. The best fits for the envelope curves of each beam were computed and compared with reference [6]. In this reference, the beam elongation is between 2~5% of the beam depth per plastic hinge.

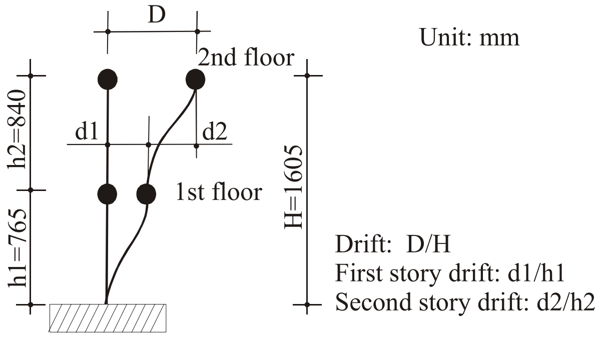

Figure 4: Definition of the used terms

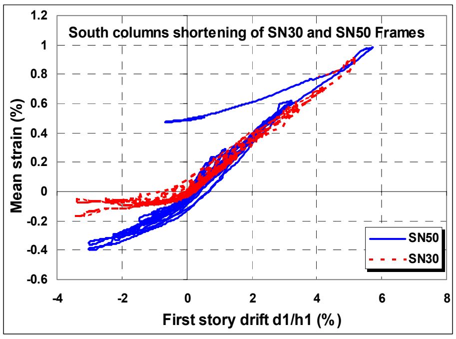

Figure 5: First story south-columns shortening

Considering that each beam had two plastic hinges, and the beam depth was 270 mm, the total calculated elongation is 11~27 mm. Using the clear beam length, the mean strain can be found to be 0.71~1.76 %. The best fit for the second floor beam of frame SN50, shown in **Figure 6**, had a mean strain of 1.59%, which is within the range given by reference [6]. Best fits for the mean strain-drift relationships, had a linear equation passing through the origin with a form $y = ax$. The "a" coefficients for frame SN30 were 0.130 and 0.246 for the first and second floor beam respectively. These values were 0.129 and 0.225 for frame SN50 that are nearly the same as those found for SN30. Taking an average of the above coefficients, the following equation can be used to evaluate the beam mean strain, ε, in the first and second floors respectively:

$$\varepsilon = 0.13(D/H) \quad and \quad \varepsilon = 0.24(D/H) \qquad (1)$$

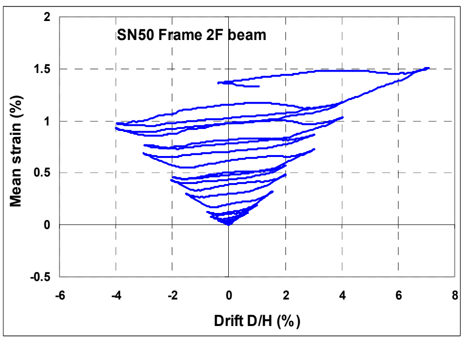

(a) Beam mean strain history

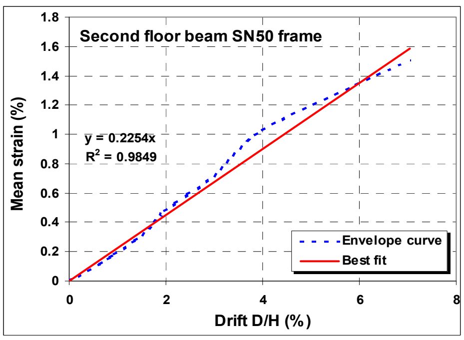

(b) Best fit for the envelope curve

Figure 6: Second floor beam mean strain SN50 frame

where D and H were introduced in **Figure 4**. An important consequence of the beam elongation is that it amplifies the column bending moment demand on one side of the frame and reduces it on the other side, due to the increase in the $P-\delta$ effect and the horizontal displacement.

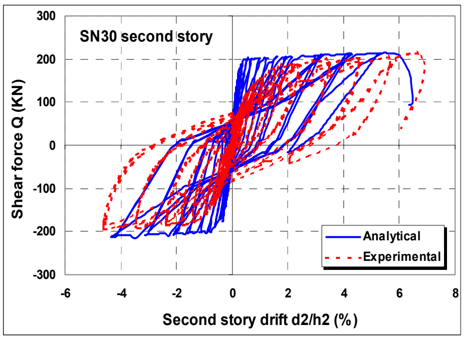

(a) Second story –SN30 frame-

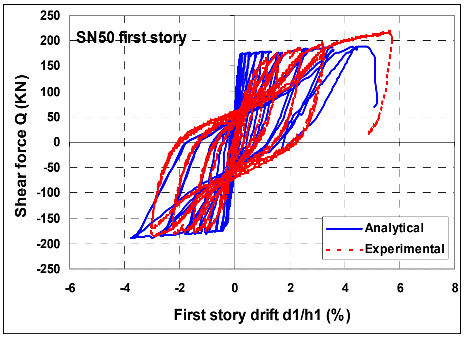

(b) First story-SN50 frame-

Figure 7: Story drift angle-shear force relation ship

3. ANALYTICAL RESULTS

Both frames were analyzed using the nonlinear program, IDARC [7]. Frames were modeled as a lumped mass with a fixed base. Rigid zones were also inserted at the columns and beams ends. The moment-curvature envelope for the frame members, were evaluated automatically using the fiber model incorporated in the program. The incremental curvature that is applied to the section is continued until the specified ultimate compressive strain in the concrete or the specified ultimate strength of one of the rebar is reached. In IDARC program, kent and Park model is used for unconfined concrete and Mander model is used for confined concrete. A simple tri-linear model is used for steel.

Figure 7 shows some typical results. At small drift ratios, the analytical stiffness exceeded the experimental stiffness due probably, to the high value of the analytical stress given by the parabola equation in the concrete model. As shown in **Figure 8**, the curvature-story drift relationship was reproduced well analytically. The experimental curvature was measured for a length equal to $D_c/2$ where D_c is the column depth. The IDARC program includes a spread plasticity formulation that can capture the change in the plastified length under single or double curvature conditions. The plastic hinge length is updated at each step in the analysis as a function of the instantaneous moment diagram in the element, but the plastic hinge length is never allowed to become smaller than the previous maximum. The experimental and the calculated curvature-story drift relationships agreed well for frame SN30 beams using a plastic-hinge length equal half of the beam height, $H_b/2$. For the first-floor beam of specimen SN50, the results that best matched the analytical curvatures were those computed using a length equal to the total beam length rather than half, as was the case for the second floor beam. In **Figure 9**, analytical and experimental results of the second floor beam of frame SN50 are compared. Due to space limitation we were unable to show all the analytical results for the frame's components, columns and beams.

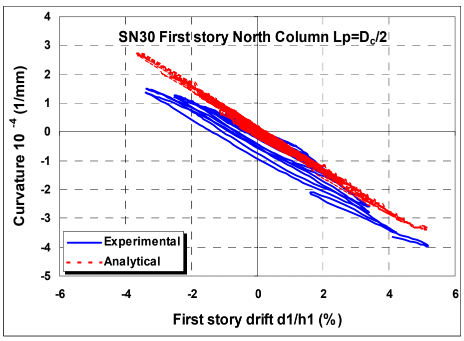

Figure 8: Curvature-story drift relationships for the first story columns

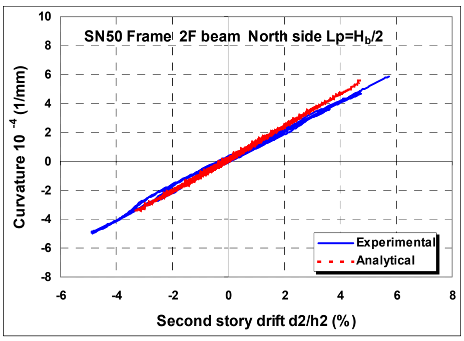

Figure 9: Beam curvature-story drift relationships -SN50 frame-

4. OBSERVED DAMAGE

As an example, **Figure 10** shows damage to SN30 frame. More cracks formed on the columns of SN50 than SN30. At 2% drift, cracks at north and south side of the first floor beam of SN30 were 1.30mm and 0.59mm, respectively. These values were 1.36mm and 2.13mm, respectively, for the second floor beam of the same frame. No buckling or severe concrete spalling was found for any columns. At the end of the test, the concrete cover located at the outside base face of the first-story column (on both the north or south sides of the frame) spalled over a length of 26 cm for frame SN50 and 15 cm for frame SN30. Even though the spacing of the transverse reinforcement was 80 mm, buckling of the longitudinal reinforcement of the second floor beams was observed on the north and south sides for both frames. Concrete of the lower part of the south side of the second floor beam crushed due to high compression; the length of the spalling was 10 cm for frame SN30 and 20 cm for frame SN50.

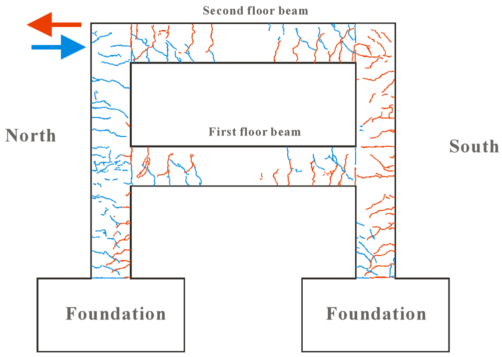

(a) Crack patter at 2% drift

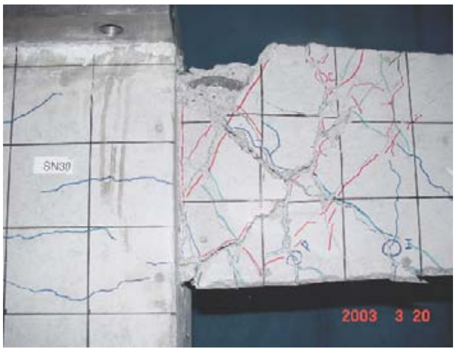

(b) Damage to the 2F beam (Buckling)

Figure 10: Observed damage to SN30 frame

5. RETROFITTING PHASE

Both frames were retrofitted by injecting epoxy resin to cracks more than 0.3 mm and by casting a new concrete at the beams damaged (plastic hinge) regions as illustrated in **Figure 11**. The epoxy-mortar and the concrete strengths that were used to replace the spalled cover concrete and the damage concrete at beam plastic hinge region were14.6 MPa and 43.5 MPa, respectively. Buckled bars at beams were cut and new bars were welded to the straight portion of the bars on the beam side, and anchored using epoxy to the column side. Specimen SN50 and SN30 showed a large strength drop in the positive cycles as shown in **Figure 13**. This may be attributed to the fact that, beyond 4% drift both frames were pushed in the positive cycles beyond 6% drift, whereas, the maximum drift that was applied in the negative cycles was 4%. Effect of axial load intensity on hysteresis loops can be seen clearly on the negative side of the cyclic loading. Frame SN50, under high axial load, showed more strength degradation than frame SN30, under moderate axial load, due principally to the damage caused to concrete before retrofitting. Energy dissipation for the original and repaired specimens were computed and compared for both frames as shown in **Figure 12**. Dissipated energy of the repaired SN30 frame was 87.54% of the original one whereas, this value was found to be 91.41% for SN50 frame.

Figure 11: Retrofitting phase

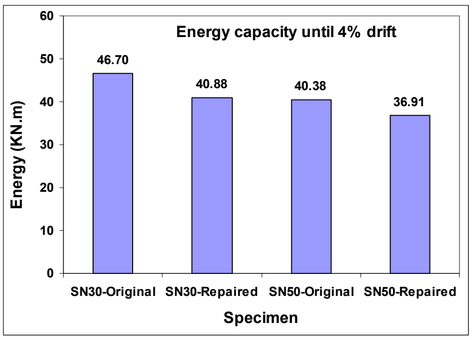

Figure 12: Energy capacity

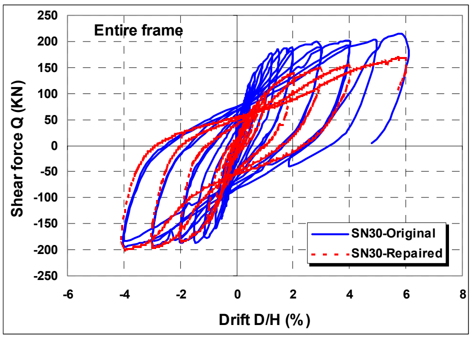

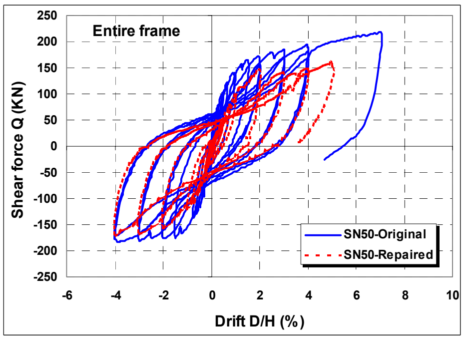

(a) SN30 frame **(b) SN50 frame**

Figure 13: Original and repaired hysteresis curves

6. CONCLUSIONS

The main conclusions of these tests and analysis can be summarized as follow:

- The overall load-displacement relationships for the stories and frames differed slightly.
- Shear forces in columns varied significantly with respect to axial load.
- Even though drift ratios of over 6% were imposed on the frames, the first and second-story columns were slightly damaged.
- The first-floor and second-floor beams were severely damaged near the beam-column joint. Even though the stirrup spacing was six times the longitudinal bar diameter, buckling of longitudinal reinforcement was observed after the concrete spalled.
- Beam elongation may increase/decrease the moment demand to columns due to the increasing/decreasing in the $P-\delta$ effect and horizontal displacement.
- Equations to predict the beams mean strain at 1^{st} and 2^{nd} floors were proposed.
- The force-displacement response of the entire frame as well as its components, columns and beams, was reproduced well using the nonlinear program, IDARC.
- Dissipated energy of repaired frames compared to the original ones, was higher for frame under high axial load than that under moderate axial load.

ACKNOWLEDGEMENT

The authors acknowledge TOPY Industries Limited, NETUREN Corporation Limited, and KOBE steel Limited for donating experimental materials. Sincere thanks are also extended to Mr. Yusaku Arai and Mr. Issei AMEMIYA, former students at Kyoto University.

REFERENCES

[1] H. Thomsen and W. Wallace, “Lateral load behavior of RC columns constructed using high-strength materials”, ACI structural journal/September-October 1994 (in English).

[2] Ang Beng Ghee, M. J. N. Priestley, and T Pauly, “Seismic shear strength of circular reinforced concrete columns”, ACI structural journal/January-February 1989 (in English).

[3] Bechtoula, H., Arai, Y., Kono, S., Watanabe, F., “Damage Assessment of RC Columns Under Large Axial and Lateral Loadings” Symposium on a design procedure of RC structures based on inelastic deformation -Use of confined concrete-, November 30, 2001, pp263-270 (in English).

[4] Kono, S., Bechtoula, H., Kaku, T., Watanabe, F., “Damage assessment of RC columns subjected to axial load and bi-directional bending” Proceeding of the Japan concrete institute Vol.24, No2, 2002, PP235-240 (in Japanese).

[5] Design guidelines for earthquake resistant reinforced concrete buildings based on inelastic concept, Architecture Institute of Japan, AIJ 1999 (in Japanese).

[6] J. Matthews, D. Bull, and J. Mander, “Investigating the load paths of floor diaphragm forces during severe damaging earthquakes”, Proc. of combined concrete society and ready mix, TR24, Rotorua, Oct. 2001: 122-31.

[7] Valles, R., E., Reinhorn, A., M., Kunnath, S., K., Li, C., Madan, A., “IDARC2D Version 4.0: A computer program for the inelastic damage analysis of buildings” Technical report NCEER-96-0010 (in English).